AD-A047 557 LEHIGH UNIV BETHLEHEM PA INST OF FRACTURE AND SOLID --ETC F/G 11/6
EFFECT OF FREQUENCY ON FATIGUE CRACK GROWTH RESPONSE OF AISI 43--ETC(U)
OCT 77 P S PAO, W WEI, R P WEI N00014-75-C-0543
UNCLASSIFIED IFSM-77-85 NL

1 OF 1
ADA047557

END
DATE FILMED
1-78
DDC

IFSM-77-85

LEHIGH UNIVERSITY

INSTITUTE OF FRACTURE AND SOLID MECHANICS

EFFECT OF FREQUENCY ON FATIGUE CRACK GROWTH RESPONSE OF AISI 4340 STEEL IN WATER VAPOR

by

P. S. Pao
W. Wei
R. P. Wei

October 1977

Technical Report No. 6
Office of Naval Research
Contract N00014-75-C-0543, NR 036-097

UNCLASSIFIED

SECURITY CLASSIFICATION OF THIS PAGE (When Data Entered)

REPORT DOCUMENTATION PAGE

READ INSTRUCTIONS BEFORE COMPLETING FORM

1. REPORT NUMBER: IFSM-77-85, TR-6

2. GOVT ACCESSION NO.

3. RECIPIENT'S CATALOG NUMBER

4. TITLE (and Subtitle): Effect of Frequency on Fatigue Crack Growth Response of AISI 4340 Steel in Water Vapor.

5. TYPE OF REPORT & PERIOD COVERED: Technical Report, No. 6

6. PERFORMING ORG. REPORT NUMBER

7. AUTHOR(s): P. S. Pao, W. Wei and R. P. Wei

8. CONTRACT OR GRANT NUMBER(s): Contract N00014-75-C-0543

9. PERFORMING ORGANIZATION NAME AND ADDRESS
Lehigh University
Bethlehem, PA. 18015

10. PROGRAM ELEMENT, PROJECT, TASK AREA & WORK UNIT NUMBERS
NR 036-097

11. CONTROLLING OFFICE NAME AND ADDRESS
Office of Naval Research
Department of the Navy
Arlington, Virginia

12. REPORT DATE
Oct 77

13. NUMBER OF PAGES
19 p.

14. MONITORING AGENCY NAME & ADDRESS (if different from Controlling Office)

15. SECURITY CLASS. (of this report)
UNCLASSIFIED

15a. DECLASSIFICATION/DOWNGRADING SCHEDULE

16. DISTRIBUTION STATEMENT (of this Report)
This document has been approved for public release and sale; its distribution is unlimited.

DDC
RECEIVED
DEC 14 1977
E

17. DISTRIBUTION STATEMENT (of the abstract entered in Block 20, if different from Report)

18. SUPPLEMENTARY NOTES

19. KEY WORDS (Continue on reverse side if necessary and identify by block number)
Fracture Mechanics, Surface Chemistry, Corrosion Fatigue, Alloy Steel, Hydrogen Embrittlement

20. ABSTRACT (Continue on reverse side if necessary and identify by block number)

The effect of cyclic load frequency on the room-temperature fatigue crack growth response of AISI 4340 steel (tempered at 205°C) in water vapor at 585 Pa (4.4 torr) has been investigated. The water vapor pressure was chosen to avoid capillary condensation at the crack tip. Crack growth tests were conducted over a frequency range from 0.1 to 10 Hz, and a range of stress intensity factors (K). The maximum K in these tests was below the apparent

DD FORM 1 JAN 73 1473 EDITION OF 1 NOV 65 IS OBSOLETE

UNCLASSIFIED 407099

SECURITY CLASSIFICATION OF THIS PAGE (When Data Entered)

threshold K for sustained-load crack growth in this environment. Fatigue crack growth rates were found to increase with the reciprocal of frequency (that is, with the period at load), and exhibited transient behavior when the test frequency was altered. By separating the growth rate into an environment independent component (pure fatigue) and an environment dependent component, it was found that the environment dependent component varied linearly with period over the frequency range 0.1 to 10 Hz. The results are correlated with the kinetics for water vapor/metal surface reactions, and with other fatigue crack growth data on high-strength steels tested in aqueous and H_2S containing environments. The frequency and transient effects are discussed in terms of possible crack-tip processes.

EFFECT OF FREQUENCY ON FATIGUE CRACK GROWTH RESPONSE OF AISI 4340 STEEL IN WATER VAPOR

P. S. Pao, W. Wei* and R. P. Wei

Lehigh University
Bethlehem, PA. 18015

The effect of cyclic load frequency on the room-temperature fatigue crack growth response of AISI 4340 steel (tempered at 205°C) in water vapor at 585 Pa (4.4 torr) has been investigated. The water vapor pressure was chosen to avoid capillary condensation at the crack tip. Crack growth tests were conducted over a frequency range from 0.1 to 10 Hz, and a range of stress intensity factors (K). The maximum K in these tests was below the apparent threshold K for sustained-load crack growth in this environment. Fatigue crack growth rates were found to increase with the reciprocal of frequency (that is, with the period at load), and exhibited transient behavior when the test frequency was altered. By separating the growth rate into an environment independent component (pure fatigue) and an environment dependent component, it was found that the environment dependent component varied linearly with period over the frequency range 0.1 to 10 Hz. The results are correlated with the kinetics for water vapor/metal surface reactions, and with other fatigue crack growth data on high-strength steels tested in aqueous and H_2S containing environments. The frequency and transient effects are discussed in terms of possible crack-tip processes.

*Now Research Assistant, Department of Metallurgy & Mining Engineering, University of Illinois at Urbana-Champaign, Urbana, Illinois 61801.

Introduction

Corrosion fatigue is a generic term that describes the cracking response of a material to the combined actions of cyclically varying loads and corrosive (aggressive) environments. It is recognized as one of the most important causes for failures in engineering structures. Characterizations of corrosion fatigue response of materials are complicated by the need to incorporate a multitude of loading variables and their interactions with a range of environments. Much of the work during the past 15 years has been directed towards examinations of the influences of environments on fatigue crack growth. The essential results from these studies have been summarized in a number of review papers and proceedings of symposia [1-4]. These results indicated that the rate of environment-enhanced fatigue crack growth is a function of stress intensity factor (maximum or range, i.e., K_{max} or ΔK), load ratio (R), cyclic load frequency (f) and waveform, fugacity (or pressure) or concentration of the aggressive environment, temperature, etc. [1-5]. The specific response also depended on the particular material-environment system, and was grouped into three categories by McEvily and Wei [2] in relation to the threshold stress intensity factor (K_{Iscc}) for stress corrosion cracking of the material.

For maximum stress intensity factors (K_{max}) above K_{Iscc}, the environmental contribution arises principally from "stress corrosion cracking" and may be determined (to a first order approximation) from sustained-load crack growth data [6]. For K_{max} below K_{Iscc}, the environmental contribution was thought to arise from synergistic action of fatigue and environmental attack [1]. In the latter case, Barsom [7] showed that the rate of fatigue crack growth in a highly alloyed steel, tested in 3.5 pct NaCl solution, depended on cyclic load frequency and waveform. The rate of crack growth was higher at the lower frequencies, and the environmental effect was nearly negligible for waveforms with a high rise-time (such as square waves). The dependence on frequency was confirmed by the results of Gallagher [8] on a HY-80 steel, again tested in 3.5 pct NaCl solution, and those of Miller et al. [9] on a low-alloy steel tested in distilled water. Frequency effect for fatigue crack growth at K_{max} below K_{Iscc} had been observed in aluminum alloys tested in water vapor (without capillary condensation at the crack tip) [10,11]. Bradshaw and Wheeler suggested that the observed frequency effect resulted from the time available for the reaction of newly produced crack surfaces with the environment [10]. In distilled water, however, aluminum alloys exhibited only minor effects of frequency [1,12] and no influence of waveform [13]. Hudak and Wei suggested that the difference in behavior between the steels and aluminum alloys may be attributed to differences in the reactivity of these alloys to water. Unfortunately, however, there were no data on surface reactions to support either of the suggestions.

In a recent study, a slow step in the reaction of water/water vapor with metal surfaces was identified as the rate controlling process for sustained-load crack growth in an AISI 4340 steel [14]. The kinetics for this reaction were also determined. Preliminary data on fatigue crack growth in water vapor had shown an effect of cyclic load frequency; no influence of frequency was observed for crack growth in an inert reference environment [15]. With these additional data, it appeared reasonable to carry out a more systematic examination of the influence of cyclic load frequency on fatigue crack growth on this steel.

In the present study, the kinetics of the environment-enhanced fatigue crack growth (corrosion fatigue) were determined on the same laboratory melted heat of AISI 4340 steel that had been used for the previous studies [14]. The interrelationship between the kinetics of water vapor-metal surface reaction and the kinetics of fatigue crack growth for this steel in water vapor was

examined. Plausible explanations for the observed fatigue crack growth response were considered. Fracture morphology was characterized by scanning electron microscopy and was correlated with the kinetic data and mechanical variables.

Material and Experimental Work

A laboratory vacuum-melted AISI 4340 steel, with extra-low residual impurities was used in this investigation*. Specimen blanks were cut from 0.9-cm-thick hot-rolled plate and were heat treated before finish machining into test specimens. Chemical composition, heat treatment and mechanical properties of this steel are given in Table 1.

Table 1

Chemical Composition, Heat Treatment, and Mechanical Properties of AISI 4340 Steel Investigated

Chemical Composition, Weight Percent

C	Mn	P	S	Si	Ni	Cr	Mo	Co	Ti
0.42	0.70	0.0009	0.0012	0.28	1.83	0.79	0.24	0.011	<0.005

Heat Treatment

Normalize, 900°C, 1 h, A.C.; Austenitize, 843°C, 1 h, O.Q.; Temper, 205°C, 1 h, A.C.

A.C. = air cool; O.Q. = oil quench

Mechanical Properties

Yield Strength (MPa)	Tensile Strength (GPa)	Young's Modulus (GPa)	Elongation (pct)
1344	2082	201	9

Modified wedge-opening-load (WOL) Specimens [16], oriented in the longitudinal (LT) direction, were used for determining the fatigue crack growth kinetics in water vapor. The specimens were 5.23 cm wide, with a half-height to width ratio (H/W) of 0.486. A crack starter notch, 1.52 cm in length with a root radius of 0.025 cm, was introduced into each specimen using electrospark discharge machining. The notch was further sharpened by fatigue in dehumidified argon immediately prior to the start of the crack growth test. Fatigue precracking and subsequent fatigue tests were carried out under sinusoidally varying loads, at a load ratio (R) of 0.1 in a closed-loop electrohydraulic testing machine operated in load control. Load accuracy was maintained to better than ± 1 pct. Cyclic load frequencies from 0.1 to 10 Hz were used to examine the influence of frequency on environment-enhanced fatigue crack growth. Frequencies of 0.1, 1 and 10 Hz were selected for the frequency cycling experiments. Changes in frequency for the frequency cycling experiments were made simply by switching the frequency range selector without interrupting the fatigue test; although the load amplitude was reduced momentarily by less than 5 pct during each frequency change to avoid "overshoot" that might be introduced by the changing dynamic response of the testing system.

*Steel was furnished by the Research Laboratory of United States Steel Corporation, Monroeville, PA.

The stress intensity factor range, ΔK, was computed from Eq. (1), which is accurate to ± 1 pct for $0.3 \leq a/W \leq 0.75$ [3].

$$\Delta K = \frac{\Delta P \sqrt{a}}{BW} Y(a/W) \qquad (1)$$

$$Y(a/W) = 30.96 - 195.8(a/W) + 730.6(a/W)^2 - 1186.3(a/W)^3 + 754.6(a/W)^4$$

ΔP = applied load range; B = specimen thickness; W = specimen width; a = crack length; and $Y(a/W)$ = geometric factor.

A continuous-recording dc electrical potential system was used to monitor crack growth [17]. The following experimental calibration relationship was used to convert electrical potential to crack length:

$$a = 1.734 + 4.619V^* - 1.180V^{*2}; \quad 0.02 \leq V^* \leq 0.48 \qquad (2)$$

where a = crack length in cm

V^* = normalized electrical potential = $(V - V_r)/V_r$

V = electrical potential corresponding to the current crack length

V_r = reference electrical potential corresponding to a crack length of 1.725 cm (0.679 in.)

Crack growth rates were determined from graphical differentiation of the potential-time records. The sensitivity of the crack monitoring system, at a working current of about 3 amp, was such that changes in crack length of about 10μm and in crack growth rate of about 2×10^{-7} cm/cycle can be readily resolved. Uncertainty in crack length measurements was estimated to be ± 1 pct, and that for crack growth rate measurements, less than ± 20 pct.

Fatigue crack growth experiments were carried out in water vapor and in dehumidified argon at room temperature. The environment was maintained along the expected crack path by the use of stainless steel chambers clamped to the specimens; the chambers being connected to a suitable gas supplying system. Dehumidified "ultra-pure" argon (99.999 pct purity), further purified by an in-line titanium sublimation pump, was used as the reference environment. Water vapor at a partial pressure of 585 Pa (4.4 torr) was selected as the aggressive environment to avoid capillary condensation at the crack tip [18]. This environment was readily obtained by flowing "ultra-pure" argon through distilled water maintained at 0°C.

Characterization of the morphology of fracture surfaces produced by environment-enhanced fatigue crack growth at the different cyclic load frequencies was made with the aid of scanning electron microscopy. The entire broken halves of selected specimens were placed inside an ETEC Auto-scan microscope for examination. By this procedure, the location on the fracture surface can be readily determined, and specific morphological features could be correlated then with the kinetic data and with the appropriate mechanical variables (such as ΔK).

Results

Effect of Cyclic Load Frequency

Fatigue Crack growth data on AISI 4340 steel, obtained under sinusoidal

loading at room temperature and a water vapor pressure of 585 Pa (4.4 torr), for various loading frequencies are shown in Fig. 1. Data from the reference (argon) environment are also included in Fig. 1 for comparison. These data cover stress intensity factor range (ΔK) from 15 to 40 MPa-$m^{1/2}$ at R = 0.1.

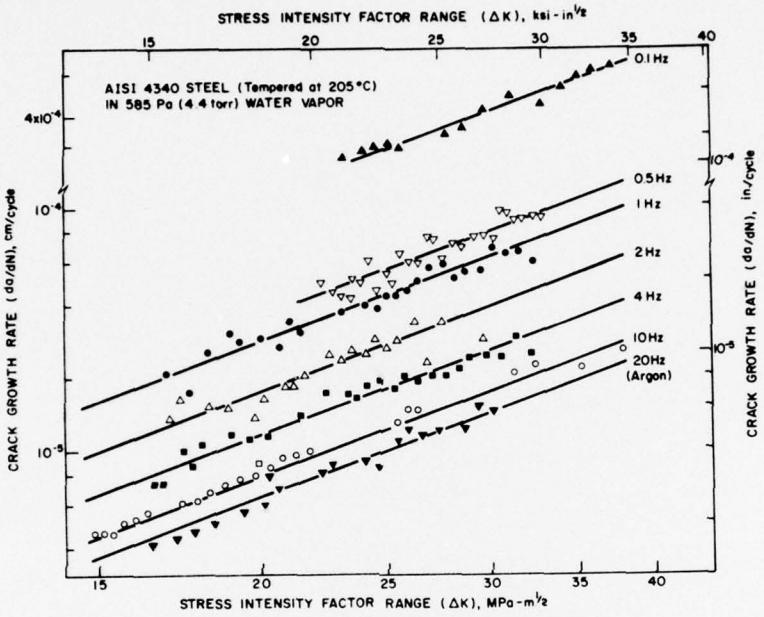

Figure 1 - Room temperature fatigue crack growth kinetics on AISI 4340 steel tested in dehumidified argon and in water vapor (below K_{Iscc}) at R = 0.1.

The corresponding maximum stress intensity factors (K_{max}) were below the apparent K_{Iscc} (approximately 55 MPa-$m^{1/2}$) for this water vapor pressure [15]. The results clearly show that water vapor increased the rate of fatigue crack growth below K_{Iscc} to a greater extent at low frequencies than at the higher frequencies. The percentage increase over the growth rate in the reference environment, at a given frequency, was essentially the same over the range of ΔK used in this investigation. In other words, data at the different frequencies followed essentially parallel curves in log (da/dN) versus log (ΔK) coordinates.

Assuming that the crack growth kinetics, over the indicated range of ΔK shown in Fig. 1, can be represented by the relationship $da/dN = C(\Delta K)^n$ [19], least-squares regression analyses of the data were made and showed that the data conformed with this relationship. The exponents n were found to be equal at 95 pct confidence level, and had a pooled value of nearly 2. For simplicity, a value of n = 2 was chosen, and the experimental data were empirically represented by Eq. (3) for use in further analyses.

$$\frac{da}{dN} = C(\Delta K)^2 \qquad (3)$$

The constant C is a dimensional constant, and was determined from each set of data by least-squares regression analysis based on Eq. (3). The constant C,

therefore, reflected the influence of frequency or period on environment-enhanced fatigue crack growth. The value corresponding to the reference data was taken to be C_o (that is, for data obtained in argon at 20 Hz).

Environment induced increase in fatigue crack growth rate may be given by the difference between crack growth rate in the aggressive environment, $(da/dN)_e$, and that in the reference environment, $(da/dN)_r$, at the same ΔK level.

$$(da/dN)_e - (da/dN)_r = (C - C_o)(\Delta K)^2 \qquad (4)$$

This increase is thus represented by $(C - C_o)$ over the entire range of ΔK investigated. The values for $(C - C_o)$ are shown as a function of the inverse of cyclic load frequency (that is, of period) in Fig. 2. Error bands in Fig. 2 represent estimates of 95 pct probability for occurrence [20]. Least-squares analysis of these data showed that $(C - C_o)$ is linearly proporational to the period (τ = 1/frequency) on a 95 pct confidence level basis. This correlation indicates that the increase in the rate of fatigue crack growth by the environment is proportional to the "time-at-load" (that is, for loads above the minimum load in a given cycle). The mechanistic implications of this finding are considered in the discussion.

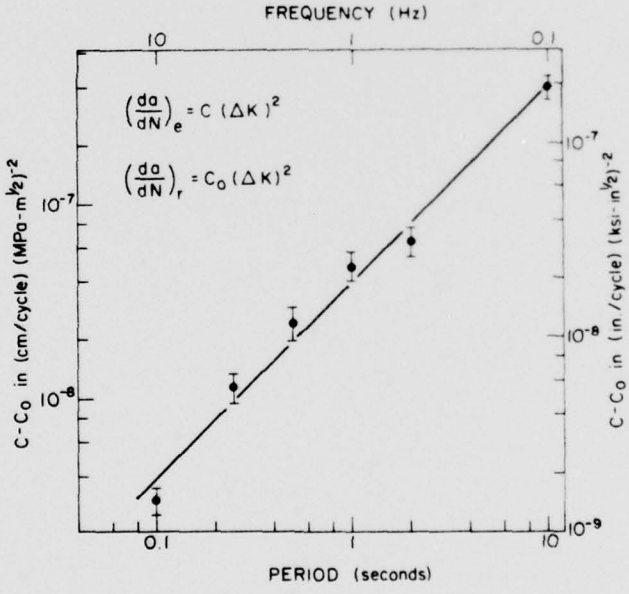

Figure 2 - Environment dependent component of fatigue crack growth parameter as a function of cyclic load period for AISI 4340 steel tested in water vapor at room temperature.

Transient Phenomenon

Changes in crack growth rate associated with changes in cyclic load frequency, for constant load-amplitude fatigue in 585 Pa (4.4 torr) water vapor at room temperature, are shown as a function of crack length in Fig. 3.

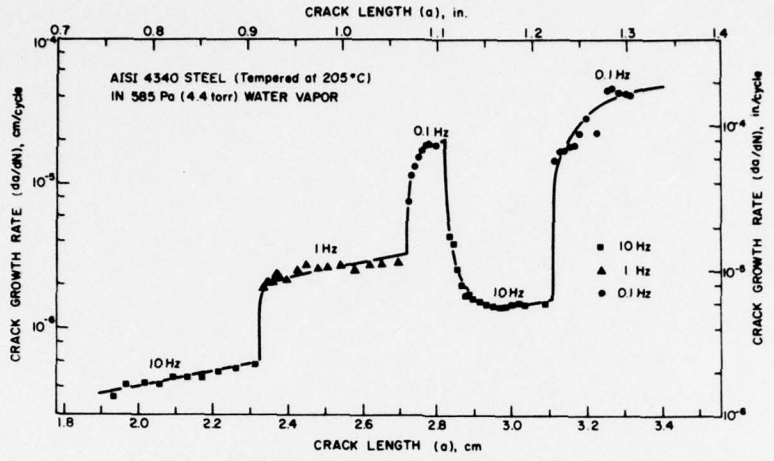

(a)

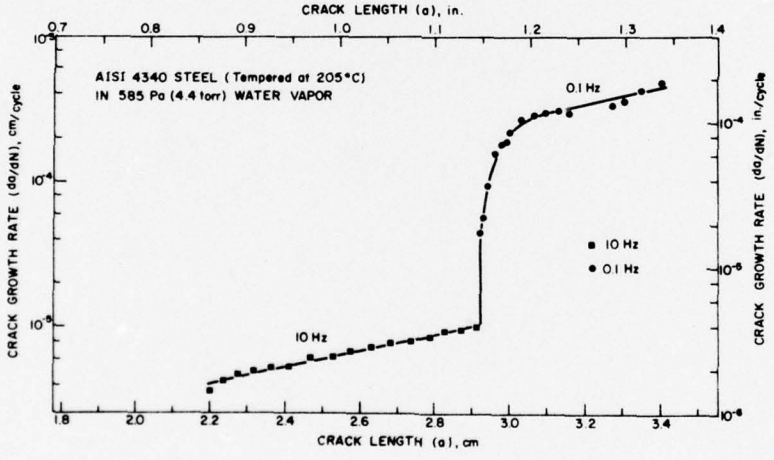

(b)

Figure 3 - Crack growth rate response resulting from changes in cyclic load frequency.

Data shown in Fig. 3a were obtained from test on a specimen that had been fatigued at 0.1. 1, and 10 Hz under the same maximum and minimum loads. Fatigue crack was extended by at least 0.25 cm (about 0.1 in.) following each change in frequency to allow steady-state rate to be established at the new test frequency. Only two test frequencies (0.1 and 10 Hz) were used for the data shown in Fig. 3b to better illustrate the transition between steady-state rates.

Data in Fig. 3 clearly show a region of transient growth, following each change in cyclic load frequency, before steady-state growth rate became established at the new frequency. For example, decreasing the frequency from 10 Hz to 0.1 Hz (see Figs. 3a and 3b) did not produce an immediate change in

crack growth rate to its expected steady-state value. Instead, it resulted in a gradual change that extended over crack growth increments of the order of 0.1 cm. Similarly, an increase in frequency (see Fig. 3a) produced a gradual decrease in growth rate to its steady-state value. The extent of crack growth required to establish steady-state growth (that is, the size of the transition zone) appeared to depend on the magnitude of the frequency change and on the crack length (or ΔK, for constant load-amplitude fatigue). Since there is no influence of frequency on fatigue crack growth in an inert environment over this range of frequencies [1,15], the observed transient phenomenon must result from interactions with the environment. The implications of this phenomenon are considered in the discussion section.

Fractography

Representative SEM microfractographs obtained from specimens tested in 585 Pa (4.4 torr) water vapor at 10 Hz and 1 Hz for ΔK of 25 MPa-$m^{1/2}$, are shown in Figs. 4a and 4b, respectively. The arrows above these figures indicate the macroscopic crack growth direction.

The features shown in Fig. 4a are typical of the fracture surface morphology for a specimen tested in water vapor at 10 Hz. The fracture mode is similar to that for specimens tested in dehumidified argon at 20 Hz at comparable ΔK levels. This similarity in fracture surface characteristics was not unexpected, inasmuch as the environmental effect was not large at this frequency. The morphology, therefore, would reflect primarily that associated with "pure" fatigue. In general, the crack path appeared to be transgranular with respect to the prior austenite grains. The crack path, however, may be intergranular with respect to martensite and twin boundaries within the prior austenite grains.

As the cyclic load frequency was reduced, the fracture appearance changed. Fracture surface morphology that was observed on specimens tested at 1 Hz, shown in Fig. 4b, is typical of that observed at the lower frequencies. The fracture path is now markedly different from that observed at 10 Hz. The most significant difference was the occurrence of a large component of intergranular separation along the prior austenite grain boundaries. Some transgranular quasi-cleavage (i.e., with respect to the prior austenite grains) and secondary cracks out of the plane of macroscopic fracture can be seen also in Fig. 4b. The difference in fracture mode between 10 Hz (Fig. 4a) and 1 Hz (Fig. 4b) was associated with approximately a 4-fold increase in crack growth rate.

Fracture morphology at frequencies below 1 Hz (Fig. 4b) was very similar to that observed on the same AISI 4340 steel tested in hydrogen and in water under sustained-load [14]. This similarity indicates that, in AISI 4340 steel, sustained-load crack growth in hydrogen and in water, and fatigue crack growth below K_{Iscc} in water vapor at the lower frequencies followed essentially the same path through the microstructure.

Discussion

Results from this study may be considered in relation to data on surface reaction kinetics on the same AISI 4340 steel. To assist in this consideration, principal results from previous investigations are briefly summarized. In these investigations [14,21,22], characterization of the kinetics of water vapor and hydrogen sulfide reaction with iron single crystal and with AISI 4340 steel surfaces as a function of temperature and exposure (pressure x time) were made with the aid of Auger electron spectroscopy (AES) and of low energy electron diffraction (LEED). Correlation with sustain-load crack

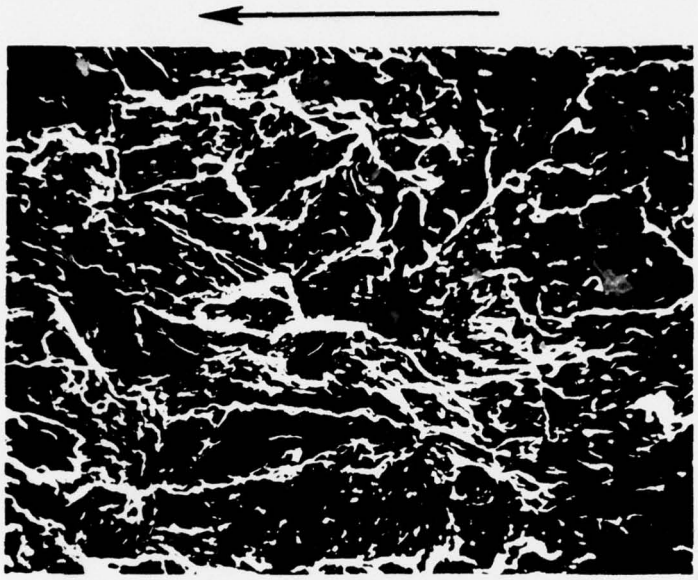

(a)

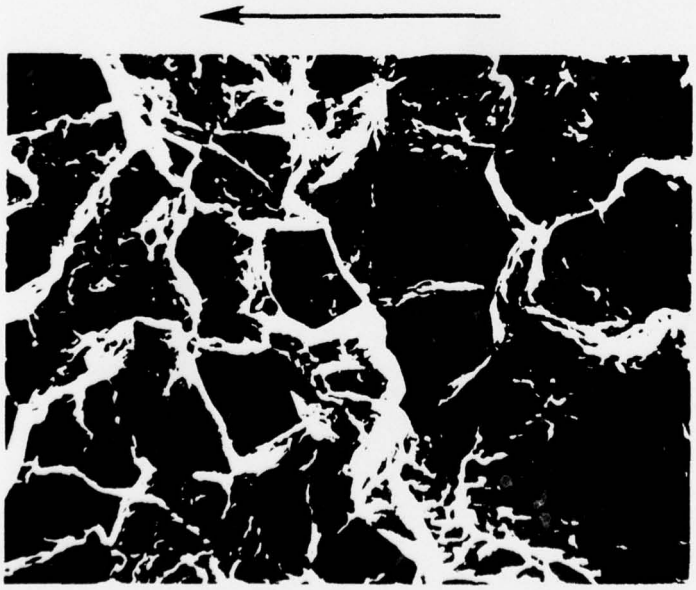

(b)

Figure 4 - Fatigue fracture surface morphology for AISI 4340 steel tested in 585 Pa (4.4 torr) water vapor at two frequencies (ΔK = 25 MPa-$m^{1/2}$): (a) 10 Hz, (b) 1 Hz.

growth response was made in the case of water/water vapor [14]. The principal findings are as follows:

(1) The initial chemisorption of water vapor on iron and on AISI 4340 steel surfaces was extremely rapid and was essentially complete in about the order of one microsecond at water vapor pressures of 0.67 to 1.06 kPa (5-8 torr). This initial step of surface reaction is not thermally activated, and was too fast to account for the observed crack growth kinetics.

(2) The second step of surface reaction, involving the formation of surface oxide and presumed production of hydrogen, required water vapor exposure on the order of 1.33 to 1.33 x 10^3 kPa-s (10 to 10^4 torr-s). This step of the reaction was thermally activated and was identified as the rate controlling process for crack growth [14]. The extent of reaction, as a function of exposure at three temperatures, is shown in Fig. 5. The solid curves represent correlation of an approximate model to the experimental data [14].

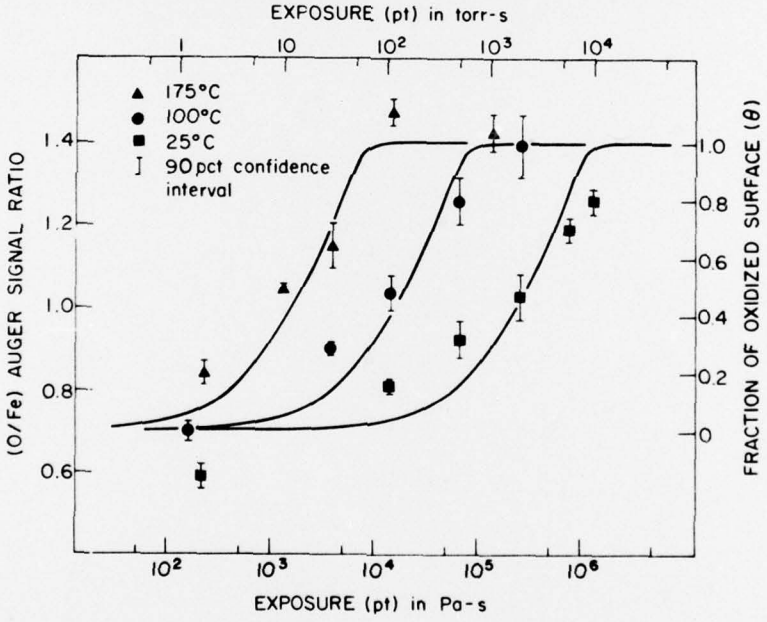

Figure 5 - Reactions of water vapor with AISI 4340 steel surface as a function of exposure at three temperatures [14].

(3) At sufficiently high exposures (above 10^6 Pa-s at room temperature) the surface oxide film would reach a limiting thickness and prevent further reaction with water vapor. The oxide layer that formed on the AISI 4340 steel surface, after saturation exposure to water vapor, was on the order of one to two atomic layers thick [14].

(4) The "slow step" in the reactions of hydrogen sulfide with AISI 4340 steel surface was about 10^6 times faster than the corresponding step for the water vapor-metal surface reaction [14].

Because hydrogen embrittlement had been identified as the mechanism for crack growth under sustained load in water and water vapor, and because water/metal surface reaction had been shown to be the rate controlling process for this growth, it is reasonable to expect that the same mechanism and rate controlling process would operate in the case of fatigue crack growth in water vapor and in aqueous environments. The similarity between fracture paths for sustained-load crack growth and for fatigue crack growth (at the lower frequencies) tends to support this expectation. Because the environment enhancement of crack growth occurred at K_{max} levels well below the threshold K (K_{Iscc}) for sustained-load crack growth, and because of the observed frequency effect and of the transient response associated with frequency changes, one would expect the embrittlement to involve a region of material ahead of the crack tip (i.e., "volume embrittlement" vis-a-vis "surface embrittlement"). The size of the embrittled, or damaged, zone would depend on the time available for reaction (viz., cyclic load period) and on the reaction kinetics.

Results obtained from this investigation suggest a conceptual model in which a steady-state zone of "embrittled" material exists ahead of the crack tip under steady-state conditions; that is, for prescribed ΔK, cyclic load frequency and environment. The conceptual model is illustrated schematically in Fig. 6. The damaged zone is depicted as circles, representing some appropriate hydrogen concentration contour ahead of the crack tip. Because more hydrogen is produced at the lower frequencies (longer exposure time), the size of the damaged zone and/or the hydrogen concentration within the zone are expected to be larger at the lower frequencies (Fig. 6). On each cycle of loading, the crack would extend, in one step, through a fraction of this zone (the detailed mechanism for this growth is not important here). Following this increment of crack growth, a steady-state zone is reestablished ahead of the new crack tip through reactions of the environment with the freshly created crack surface, and hydrogen diffusion and redistribution.

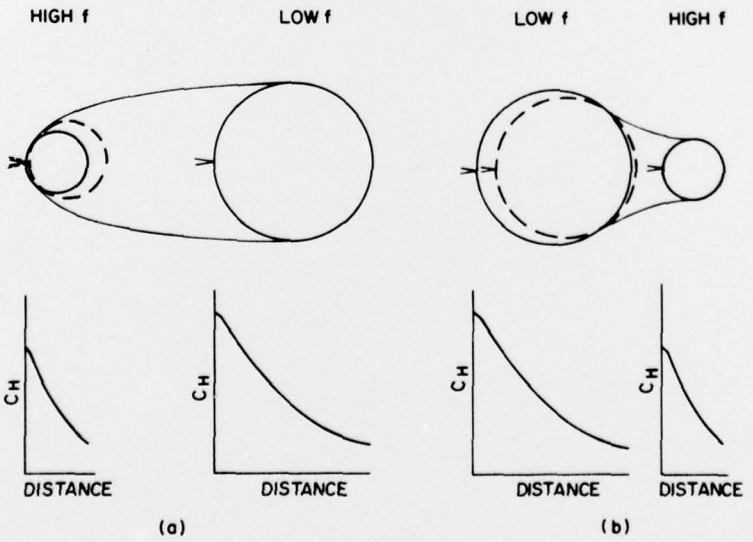

Figure 6 - Schematic illustration of conceptual model for environment assisted fatigue crack growth below K_{Iscc}.

The existence of environmental effects at K_{max} levels below K_{Iscc} for fatigue is not inconsistent with the definition of K_{Iscc} for sustained loading, since fatigue is a more proficient process for producing fresh surfaces to react with environment and to produce subsequent embrittlement. The consistency of this conceptual model in terms of experimental observations on frequency and transient effects and of surface reaction kinetics is discussed in the following sections.

Frequency Effect

For the purpose of discussion, the fraction of the surface converted to oxide (θ) and the normalized surface reaction rate, for the reaction of water vapor with AISI 4340 steel, as a function of exposure (pt) at room temperature are shown in Fig. 7. The curves are based on an approximate kinetic model for the oxidation reaction [14], and may be regarded as a schematic representation of the reaction. According to the conceptual model for fatigue crack growth, water molecules in the environment will undergo dissociative chemical reaction with the freshly produced crack surfaces to release hydrogen. The amount of hydrogen produced, at a given vapor pressure, depends on the time allowed for this reaction to take place during each fatigue cycle and on the extent of available fresh surfaces. All or a part of the hydrogen thus generated diffuses into the steel and is expected to segregate to the region of high triaxial tensile stress near the crack tip. This segregation of hydrogen embrittles the material and enhances fatigue crack growth by one or more of the hydrogen embrittlement mechanisms [23-26]. The actual mechanism of this embrittlement remains to be determined, but is not important for the present discussion.

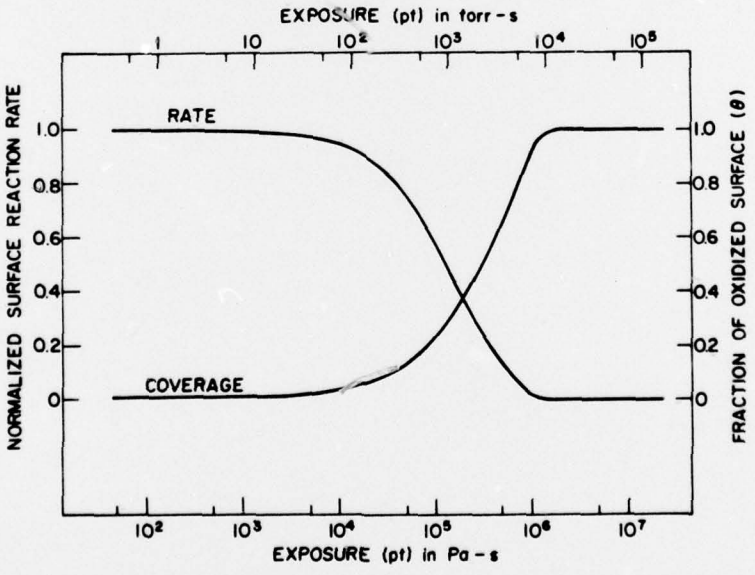

Figure 7 - Extent and normalized rate of reaction of water vapor with AISI 4340 steel surface as a function of exposure at 25°C [14].

This conceptual model appears to be consistent with the experimental data on crack growth kinetics and with the kinetics of surface reactions (see Figs. 2,6 and 7). At frequencies of 0.1 to 10 Hz and a water vapor pressure of 585 Pa (4.4 torr) used in this investigation, the freshly produced crack

surfaces were subjected to exposures of up to 58.5 to 5850 Pa-s (0.44 to 44 torr-s) per cycle. In this exposure range, the surface reaction rate or rate of hydrogen production were essentially equal (Fig. 7). Thus, the environmental contribution to the rate of fatigue crack growth, $(da/dN)_e - (da/dN)_r$ or $(C - C_o)$, would be expected to be essentially proportional to the cyclic-load period (1/frequency). This expectation is consistent with the observed frequency dependence shown in Fig. 2.

Data on the kinetics of water vapor/AISI 4340 steel surface reaction [14] (see Fig. 5) suggested that the initiation of the second step of reaction (leading to the production of hydrogen) at room temperature occurred at a fairly high exposure; estimated to be about 13.3 Pa-s (10^{-1} torr-s). For this AISI 4340 steel tested in 585 Pa (4.4 torr) water vapor, no environmental effect would be expected above a test frequency of about 50 Hz (period of 0.02 s). On the other hand, at exposures above 10^6 Pa-s (10^4 torr-s), the oxidation of the steel surface is essentially complete and no further hydrogen production takes place. The crack growth rates are expected to reach a saturation value and exhibit no frequency dependence. The general trend suggested by the conceptual model, at the lower frequencies, is consistent with data reported by Gallagher [8] for fatigue crack growth in HY-80 steel in 3.5 pct NaCl solution (Fig. 8). The overall trend is also in agreement with

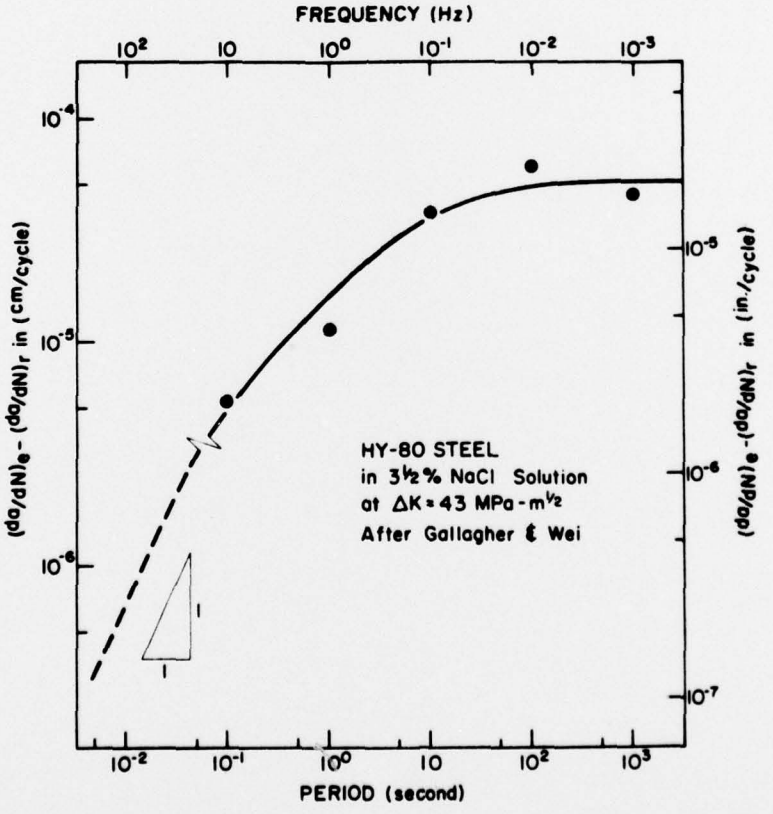

Figure 8 - Environment dependent component of fatigue crack growth rate as a function of cyclic load period for HY-80 steel tested in 3.4% NaCl solution at room temperature [8].

the results of Bradshaw and Wheeler [10] for fatigue crack growth in aluminum alloys in water vapor (without capillary condensation at the crack tip). Indeed the rationale is consistent with that proposed by Bradshaw and Wheeler [10]. Unfortunately surface reaction data for aluminum and aluminum alloys are still not available to allow for more direct comparisons.

Vosikovsky [27] explored the influences of changes in both stress intensity factor range and frequency on the below K_{Iscc} corrosion fatigue crack growth behavior of an X65 line pipe steel in sour crude oil. In his investigation, crude oil containing H_2S of about 1 ppm and 4700 ppm (saturation concentration) was used, and cyclic frequencies ranging from 0.1 to 10 Hz were considered. The maximum increase in growth rate relative to that in air was observed to be about 3 times at low H_2S concentration, and about 20 times at saturation concentration. Some frequency dependence was observed at low H_2S concentration. There was, however, essentially no frequency effect at the higher H_2S level. The absence of frequency effect at high H_2S concentration is not surprising and is consistent with the conceptual model in light of results that showed H_2S to react about 10^6 times faster and to reach saturation 10^6 times sooner than H_2O with iron and AISI 4340 steel surfaces [14,22]. The results at low H_2S concentration are less clear and may have been affected by the presence of water (about 0.3 pct) in the crude oil [27].

Transient Phenomenon

The observed transient phenomenon is consistent with the suggested conceptual model (see Fig. 6). According to this model, the size of the damaged zone and/or the hydrogen concentration within the zone are expected to be smaller at high frequencies than that at the lower frequencies. When the frequency is decreased, say from 10 Hz to 0.1 Hz, the crack initially encounters the small damage zone corresponding to steady state crack growth at the initial higher frequency. A small increment of crack growth, therefore, would result during the first load cycle at the new frequency. The time available for surface reaction after this increment of growth, however, is now much longer. The size of the damage zone would then be expected to become larger than its original size, and a larger increment of crack growth would result on the subsequent cycle of loading. Crack growth would proceed thereafter in successively larger increments until the steady state crack growth rate and damage zone size, corresponding to the lower frequency, are established. This process is illustrated schematically in Fig. 6a Conversely, the reverse process is expected to occur with an increase in frequency, see Fig. 6b.

The concept of "volume embrittlement" is essential in constructing the suggested conceptual model. Otherwise, it would be difficult to account for the observed transient phenomenon.

Summary

The effect of cyclic load frequency on the room-temperature fatigue crack growth response of AISI 4340 steel (tempered at 205°C) in water vapor at 585 Pa (4.4 torr) was investigated. The water vapor pressure had been chosen to preclude capillary condensation at the crack tip. Crack growth tests were conducted over a frequency range from 0.1 to 10 Hz, and stress intensity factor range (ΔK) from 15 to 40 MPa-$m^{1/2}$ (at a load ratio R of 0.1). The corresponding K_{max} levels were below the K_{Iscc} of 55 MPa-$m^{1/2}$ for this environment. The principal findings of this investigation are as follows:

(1) There was a significant effect of cyclic load frequency on the rate of fatigue crack growth in water vapor. The rate of crack growth

for the prescribed conditions, may be represented by an empirical relationship

$$\frac{da}{dN} = C(\Delta K)^2$$

(2) The rate of fatigue crack growth may be separated into an environment independent and an environment dependent component. Over the range of ΔK used in this investigation, these components may be represented by C_o and $C_1 = C - C_o$ respectively. C_1 was found to be inversely proportional to frequency (f) or to be directly proportional to period ($\tau = 1/f$) over the frequency range from 0.1 to 10 Hz.

(3) Transient crack growth, associated with a change in cyclic load frequency, was observed. Transient growth persisted over distances on the order of 0.1 cm; these distances being dependent on the magnitude of the frequency change and of ΔK.

(4) The results are consistent with a conceptual model involving crack growth through a portion of a "damaged" zone ahead of the crack tip during each cycle of loading; the mechanism for damage being that of hydrogen embrittlement. The size of this zone would depend on the time available for reaction (cyclic load period) and the surface reaction kinetics. The conceptual model is also consistent with other data in the literature, and suggests that the environment dependent component would be proportional to the extent of surface reaction per load cycle.

(5) The morphology of fractured surface is very sensitive to the cyclic frequency in water vapor. At high frequencies, the fractures are predominantly transgranular and are comparable to specimens tested in argon. The fracture surfaces of the specimens tested at low frequencies, however, exhibit predominantly intergranular separation along prior austenite grain boundaries. The intergranular fractures are consistent with those observed for sustained-load crack growth, and tend to support the identical nature of the embrittlement mechanism for these two loading conditions.

Acknowledgement

This work was supported by the Office of Naval Research under Contract N00014-75-C-0543, NR 036-097. The authors wish to acknowledge Dr. G. W. Simmons for his helpful discussion and Mr. C. D. Miller for his assistance in the experimental part of this study. The authors are grateful to the United States Steel Corporation for providing the AISI 4340 steel used in this investigation.

References

1. R. P. Wei: J. Engr. Frac. Mech., 1970, Vol. 1, p. 633.

2. A. J. McEvily and R. P. Wei: Corrosion Fatigue, ed. O. Devereux, A. J. McEvily and R. W. Staehle, 1971, p. 381, NACE, Houston, Texas.

3. Corrosion Fatigue, NACE, Houston, Texas, 1971.

4. Fatigue Crack Propagation, ASTM STP 415, Am. Soc. Testing Matls., Philadelphia, Pennsylvania, 1967.

5. R. P. Wei and M. O. Speidel: Corrosion Fatigue, ed. O. Devereux, A. J. McEvily and R. W. Staehle, 1971, p. 379, NACE, Houston, Texas.

6. R. P. Wei and J. D. Landes: Matls. Res. Std., 1969, Vol. 9, p. 25.

7. J. M. Barsom: Corrosion Fatigue, ed. O. Devereux, A. J. McEvily and R. W. Staehle, 1971, p. 424, NACE, Houston, Texas.

8. J. P. Gallagher and R. P. Wei: Corrosion Fatigue, ed. O. Devereux, A. J. McEvily and R. W. Staehle, 1971, p. 409, NACE, Houston, Texas.

9. G. A. Miller, S. J. Hudak and R. P. Wei: J. Testing and Evaluation, 1973, Vol. 1, p. 524.

10. F. J. Bradshaw and C. Wheeler: RAE Tech. Report No. 68041, 1968.

11. A. Hartman, F. J. Jacobs, A. Nederveen and R. DeRijk: NLR Tech. Note No. M2181, 1967.

12. R. P. Wei: J. Frac. Mech., 1968, Vol. 4, p. 159.

13. S. J. Hudak and R. P. Wei: Corrosion Fatigue, ed. O. Devereux, A. J. McEvily and R. W. Staehle, 1971, p. 433, NACE, Houston, Texas.

14. G. W. Simmons, P. S. Pao and R. P. Wei: Submitted for publication to Met. Trans.

15. J. P. Hutin: M.S. Thesis, Lehigh University, 1975.

16. W. K. Wilson: Westinghouse Research Laboratories, Report No. 67-707-BTLPV-R1, 1967.

17. C. Y. Li and R. P. Wei: Matls. Res. Std., 1966, Vol. 6, p. 392.

18. H. H. Johnson and A. M. Willner: Appl. Mater. Res., 1965, Vol. 4, p. 34.

19. P. C. Paris and F. Erdogan: Trans. ASME, 1963, Vol. 85, p. 528.

20. W. G. Clark and S. J. Hudak: J. Testing and Evaluation, 1975, Vol. 3, p. 454.

21. D. J. Dwyer, G. W. Simmons and R. P. Wei: Surface Sci., 1977, Vol. 64, p. 617.

22. D. J. Dwyer: Ph.D. Dissertation, Lehigh University, 1976.

23. C. A. Zapffe and C. E. Sims: Trans. AIME, 1941, Vol. 145, p. 225.

24. N. J. Petch and P. Stables: Nature, 1952, Vol. 169, p. 842.

25. A. R. Troiano: Trans. ASM, 1959, Vol. 52, p. 54.

26. C. D. Beachem: Met. Trans., 1972, Vol. 3, p. 437.

27. O. Vosikovsky: Corrosion, 1976, Vol. 32, p. 472.

BASIC DISTRIBUTION LIST October 197

Technical and Summary Reports

Organization	No. of Copies
Defense Documentation Center Cameron Station Alexandria, Virginia 22314	(12)
Office of Naval Research Department of the Navy	
Attn: Code 471	(1)
Code 102	(1)
Code 470	(1)
Commanding Officer Office of Naval Research Branch Office 495 Summer Street Boston, Massachusetts 02210	(1)
Commanding Officer Office of Naval Research Branch Office 536 South Clark Street Chicago, Illinois 60605	(1)
Office of Naval Research San Francisco Area Office 760 Market Street, Room 447 San Francisco, California 94102 Attn: Dr. P. A. Miller	(1)
Naval Research Laboratory Washington, D.C. 20390	
Attn: Code 6000	(1)
Code 6100	(1)
Code 6300	(1)
Code 6400	(1)
Code 2627	(1)
Naval Air Development Center Code 302 Warminster, Pennsylvania 18974 Attn: Mr. F. S. Williams	(1)
Naval Air Propulsion Test Center Trenton, New Jersey 08628 Attn: Library	(1)

Organization	No. of Copies
Naval Construction Batallion Civil Engineering Laboratory Port Hueneme, California 93043 Attn: Materials Division	(1
Naval Electronics Laboratory Center San Diego, California 92152 Attn: Electron Materials Sciences Division	(1
Naval Missile Center Materials Consultant Code 3312-1 Point Mugu, California 93041	(1
Commanding Officer Naval Surface Weapons Center White Oak Laboratory Silver Spring, Maryland 20910 Attn: Library	(1
David W. Taylor Naval Ship R&D Center Materials Department Annapolis, Maryland 21402	(1
Naval Undersea Center San Diego, California 92132 Attn: Library	(
Naval Underwater System Center Newport, Rhode Island 02840 Attn: Library	(
Naval Weapons Center China Lake, California 93555 Attn: Library	(
Naval Postgraduate School Monterey, California 93940 Attn: Mechanical Engineering Dept.	(
Naval Air Systems Command Washington, D.C. 20360	
Attn: Code 52031	(
Code 52032	(
Code 320	(

Organization	No. of Copies
Naval Sea System Command Washington, D.C. 20362 Attn: Code 035	(1)
Naval Facilities Engineering Command Alexandria, Virginia 22331 Attn: Code 03	(1)
Scientific Advisor Commandant of the Marine Corps Washington, D.C. 20380 Attn: Code AX	(1)
Naval Ship Engineering Center Department of the Navy CTR BG #2 3700 East-West Highway Prince Georges Plaza Hyattsville, Maryland 20782 Attn: Engineering Materials and Services Office, Code 6101	(1)
Army Research Office Box CM, Duke Station Durham, North Carolina 27706 Attn: Metallurgy & Ceramics Div.	(1)
Army Materials and Mechanics Research Center Watertown, Massachusetts 02172 Attn: Res. Programs Office (AMXMR-P)	(1)
Air Force Office of Scientific Research Bldg. 410 Bolling Air Force Base Washington, D.C. 20332 Attn: Chemical Science Directorate Electronics and Solid State Sciences Directorate	(1) (1)
Air Force Materials Lab (LA) Wright-Patterson AFB Dayton, Ohio 45433	(1)

Organization	No. of Copies
NASA Headquarters Washington, D.C. 20546 Attn: Code RRM	(1)
NASA Lewis Research Center 21000 Brookpark Road Cleveland, Ohio 44135 Attn: Library	(1)
National Bureau of Standards Washington, D.C. 20234 Attn: Metallurgy Division Inorganic Materials Division	(1) (1)
Defense Metals and Ceramics Information Center Battelle Memorial Institute 505 King Avenue Columbus, Ohio 43201	(1).
Director Ordnance Research Laboratory P.O. Box 30 State College, Pennsylvania 16801	(1)
Director Applied Physics Laboratory University of Washington 1013 Northeast Fortieth Street Seattle, Washington 98105	(1)
Metals and Ceramics Division Oak Ridge National Laboratory P.O. Box X Oak Ridge, Tennessee 37380	(1)
Los Alamos Scientific Laboratory P.O. Box 1663 Los Alamos, New Mexico 87544 Attn: Report Librarian	(1)
Argonne National Laboratory Metallurgy Division P.O. Box 229 Lemont, Illinois 60439	(1)

Organization	No. of Copies	Organization	No. of Copies
Brookhaven National Laboratory Technical Information Division Upton, Long Island New York 11973 Attn: Research Library	(1)		
Library Building 50 Room 134 Lawrence Radiation Laboratory Berkeley, California	(1)		

C
July 1977

SUPPLEMENTARY DISTRIBUTION LIST

Technical and Summary Reports

Dr. T. R. Beck
Electrochemical Technology Corporation
10035 31st Avenue, NE
Seattle, WA 98125

Professor I. M. Bernstein
Carnegie-Mellon University
Schenley Park
Pittsburgh, PA 15213

Professor H. K. Birnbaum
University of Illinois
Department of Metallurgy
Urbana, IL 61801

Dr. Otto Buck
Rockwell International
1049 Camino Dos Rios
P.O. Box 1085
Thousand Oaks, CA 91360

Dr. David L. Davidson
Southwest Research Institute
8500 Culebra Road
P.O. Drawer 28510
San Antonio, TX 78284

Dr. D. J. Duquette
Department of Metallurgical Engineering
Rensselaer Polytechnic Institute
Troy, NY 12181

Professor R. T. Foley
The American University
Department of Chemistry
Washington, DC 20016

Mr. G. A. Gehring
Ocean City Research Corporation
Tennessee Avenue & Beach Thorofare
Ocean City, NJ 08226

Dr. J. A. S. Green
Martin Marietta Corporation
1450 South Rolling Road
Baltimore, MD 21227

Professor R. H. Heidersbach
University of Rhode Island
Department of Ocean Engineering
Kingston, RI 02881

Professor H. Herman
State University of New York
Material Sciences Division
Stony Brook, NY 11794

Professor J. P. Hirth
Ohio State University
Metallurgical Engineering
Columbus, OH 43210

Dr. D. W. Hoeppner
University of Missouri
College of Engineering
Columbia, MO 65201

Dr. E. W. Johnson
Westinghouse Electric Corporation
Research and Development Center
1310 Beulah Road
Pittsburgh, PA 15235

Dr. F. Mansfeld
Rockwell International Science Center
1049 Camino Dos Rios
P.O. Box 1085
Thousand Oaks, CA 91360

Professor A. E. Miller
University of Notre Dame
College of Engineering
Notre Dame, IN 46556

Dr. Jeff Perkins
Naval Postgraduate School
Monterey, CA 93940

Professor H. W. Pickering
Pennsylvania State University
Department of Material Sciences
University Park, PA 16802

C
July 1977

SUPPLEMENTARY DISTRIBUTION LIST
(Continued)

Dr. William R. Prindle
National Academy of Sciences
National Research Council
2101 Constitution Avenue
Washington, DC 20418

Professor R. W. Staehle
Ohio State University
Department of Metallurgical Engineering
Columbus, OH 43210

Dr. Barry C. Syrett
Stanford Research Institute
333 Ravenswood Avenue
Menlo Park, CA 94025

Dr. R. P. Wei
Lehigh University
Institute for Fracture and
Solid Mechanics
Bethlehem, PA 18015

Professor H. G. F. Wilsdorf
University of Virginia
Department of Materials Science
Charlottesville, VA 22903